



Tuning photovoltaic performance of DOBT-based dyes via molecular design with ethynyl-linker and terminal electron-donating segment



Lihui Wang^{a, b}, Lunxiang Yin^a, Lijuan Wang^a, Bao Xie^a, Changyan Ji^a, Yanqin Li^{a, *}

^a School of Chemistry, Dalian University of Technology, Linggong Road 2, Dalian, 116024, China

^b College of Chemistry and Chemical Engineering, Inner Mongolia University for Nationalities, Tongliao, 028023, China

ARTICLE INFO

Article history:

Received 29 August 2016

Received in revised form

17 January 2017

Accepted 18 January 2017

Available online 19 January 2017

Keywords:

Benzothiadiazole

Ethynyl

Carbazole

Triphenylamine

Photovoltaic performance

Bulk heterojunction

ABSTRACT

Two novel D- π -A- π -D-typed dioctyloxy-benzothiadiazole (DOBT)-based small molecules (SMs), **TPAEDOBT** and **CZEDOBT**, were designed and synthesized, consisting of ethynyl as π -linkage, besides, incorporating triphenylamine (TPA) and alkylated-carbazole (Cz) as terminal electron-donating units respectively. Single-bond compounds, **TPADOBT** and **CZDOBT**, were designed as references to fully investigate their photovoltaic (PV) performance of solution-processed devices. As expected, the PV properties were finely tuned via molecular design with ethynyl-linker and terminal electron-donating units. Among them, the best power conversion efficiency (PCE) of 3.21% was obtained for **TPAEDOBT**-based device due to triple-bond effect and high hole-mobility. Most importantly, a remarkably increased open-circuit voltage (V_{oc}) of 1.06 V was achieved for **CZEDOBT**-based device due to synergistic effect of ethynyl-linker with electron-withdrawing character and Cz unit with the relatively weakened electron-donating ability, which is among the earliest report for DOBT-Cz based SMs with high V_{oc} so far. These results provide an important guide for rational design of novel SMs PV materials.

© 2017 Elsevier Ltd. All rights reserved.

1. Introduction

Organic photovoltaics (OPV) have been intensively investigated during the past decade due to their advantages of low production costs, high mechanical flexibility, light weight, and simplified fabrication [1]. To date, polymer based bulk heterojunction (BHJ) organic solar cells (OSCs) have reached PCEs in excess of 10% in single-junction devices [2]. In the meanwhile, solution processed SMs based OSCs have made a rapid improvement due to the intrinsic benefits of easier chemical modification, well-defined molecular structure and good reproduction [3]. Several SMs-OPV materials with PCEs near 10% have been achieved [4]. In particular, a remarkable PCE of 10.10% has been reported by Chen group [5], which is comparable with their polymer counterparts. It is worth mentioning that these intrinsic characteristics and the rapid development have made organic SMs become an excellent candidate for OPV materials [6].

Developing rational donor- π -acceptor (D- π -A) conjugated SMs is the key to high performance, because high quality D- π -A architecture can not only efficiently reduce the energy band gap (E_g), but

also well control the energy levels [7]. Therefore, the design of SMs containing appropriate D and A units provide a pathway to modulate PV properties of materials [8]. Among a variety of methods for improving V_{oc} of OPV device, modification of π -bridge in the backbone of SMs is an effective approach [9]. For instance, Li et al. have reported that a typical compound BDCTFBT with acrylonitrile-linkage exhibited an impressive V_{oc} of 1.11 V [10]. Among many studies, ethynyl-linker based SMs have received great attention owing to the intrinsic characteristics of materials, which include improved coplanarity, rigidity and electron-withdrawing character [11]. Moreover, SMs with ethynyl-linkage have the potential to improve V_{oc} owing to a deep highest occupied molecular orbital (HOMO) level [12]. However, the BHJ OPV devices with V_{oc} over 1.0 V were seldom reported by using the ethynyl-based SMs as a donor [13]. In this paper, TPA and Cz units were selected as terminal groups due to their prominent electron-donating character and good charge transportation capacity [14]. On the other hand, DOBT was designed as central acceptor unit due to its excellent solution compatibility and strong electron-withdrawing ability [15]. Although great attention has been paid to TPA, Cz and BT by reason of their advantages for OSCs, DOBT-ethynyl-TPA based D- π -A- π -D typed SMs with PCEs over 2% were seldom reported [11a,13]. Furthermore, DOBT-ethynyl-Cz based SMs have never been studied.

* Corresponding author.

E-mail address: liyanqin@dlut.edu.cn (Y. Li).

Therefore, it is highly desired to develop the synergistic effect of ethynyl-linker and electron-donating units (TPA and Cz), which will be important for tuning the OPV performance via molecular design.

In this work, two new DOBT-based SMs, **TPAEDOBT** and **CZE-DOBT**, were synthesized successfully, consisting of ethynyl as π -bridge, besides, incorporating TPA and Cz as terminal electron-donating units, respectively. In order to fully investigate the synergistic effect of π -linker and donor unit, two single-bond compounds named **TPADOBT** and **CZDOBT** were designed as reference materials. Molecular design strategy and chemical structures of these materials are shown in Scheme 1. Independent and synergistic effects of π -linker and D units were investigated systematically. As a consequence, the OPV properties were finely tuned via molecular design with ethynyl-linker and terminal electron-donating units.

2. Experimental section

2.1. Reagent and materials

All reagents and chemicals were obtained commercially and used as received unless specified. Toluene and tetrahydrofuran (THF) were pretreated by distillation over Na/benzophenone under nitrogen (N_2) atmosphere prior to use. All reactions and manipulations were performed under N_2 atmosphere with a standard Schlenk line unless otherwise noted.

2.2. Device fabrication

Solution processed OPV devices were fabricated with a conventional configuration of ITO/PEDOT:PSS/SMs-donor:PC₆₁BM/Au. The ITO-coated glass substrate was cleaned in water, methanol, acetone, toluene and isopropyl alcohol for 10 min, successively. Then a thin layer of poly(3,4-ethylenedioxythiophene):poly(styrene sulfonate) (PEDOT:PSS) was spin-coated onto the substrate at 4000 rpm s⁻¹ for 60 s. After being baked at 140 °C for 20 min, the prepared substrates were transferred into a N_2 -filled glove box. Subsequently, the active layer with a blend solution of SMs-donor and PC₆₁BM (total concentration of 12 mg mL⁻¹) was spin-coated on the top of prepared ITO/PEDOT:PSS substrate at 1500 rpm s⁻¹ for 60 s. Finally, an aluminium layer was deposited by thermal evaporation under vacuum (ca. 10⁻⁴ Pa) through a mask, yielding eight individual devices with 5 mm² effective area. The devices for hole mobility measurement were fabricated with an architecture of ITO/PEDOT:PSS/SMs-donor:PC₆₁BM/Au.

2.3. Measurements and characterization

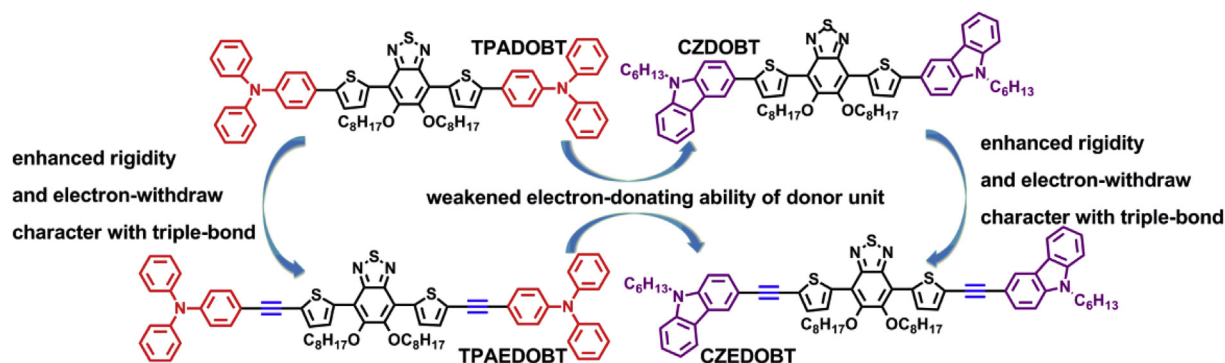
¹H NMR and ¹³C NMR spectra were measured with a Bruker

AVANCE II 400-MHz spectrometer using CDCl₃ as solvent and TMS as the internal standard. High-resolution mass spectra (HRMS) were collected with a MALDI Micro MX spectrometer. The UV–Visible absorption spectra of the synthesized materials were obtained with an Agilent Cary 5000 spectrophotometer. Fluorescence emission spectra and fluorescence quenching experiments were performed on a Shimadzu RF-5301PC spectrofluorometer. Cyclic voltammetry (CV) measurements were conducted using a CHI610D electrochemical workstation from CH instrument, Inc., it was recorded in 0.1 M anhydrous CH₂Cl₂/Bu₄NBF₄ solution under N_2 atmosphere, and ferrocene-ferrocenium (Fc/Fc⁺) couple was selected as internal standard. The glass-carbon electrode was employed as the working electrode, while Ag/Ag⁺ electrode (Ag in 0.1 M AgNO₃ solution of MeCN) and platinum wire electrode were served as the reference and the counter electrode, respectively. The corresponding energy levels (HOMO^{CV} and LUMO^{CV}) and the electrochemical band gaps (E_g^{CV}) could be obtained from onset oxidation potentials (E_{ox}) and onset reduction potentials (E_{red}) according to following empirical equations [16]: LUMO^{CV}/HOMO^{CV} = - [$E_{red/ox}$ - $E_{1/2}^{ferrocene}$ + 4.8] eV and E_g^{CV} = LUMO^{CV} - HOMO^{CV}, where E_{ox} and E_{red} are the measured onset potentials relative to Ag/Ag⁺, $E_{1/2}^{ferrocene}$ = 0.05 eV versus Ag/Ag⁺. Thermogravimetric analysis (TGA) was performed under N_2 atmosphere with a heating rate of 10 °C min⁻¹ using a TA Instruments-Q50 thermogravimetric analyzer. The current density-voltage (J - V) curves of OPV devices were recorded with a Keithley 2400 Source Measure Unit under the simulated AM 1.5 G illumination with an intensity of 100 mW cm⁻², calibrating with the standard silicon solar cell. The monochromatic incident-photon-to-electron conversion efficiency (IPCE) spectra were collected using a SM-25 photoelectric conversion analyzer. The hole mobility (μ_h) measurements were conducted in the dark with a computer-controlled Keithley 2400 Source Measure Unit system. The μ_h values can be derived by fitting the J - V curves to a space-charge-limited currents (SCLC) model in a double logarithmic scale according to the Mott-Gurney law [16]: $J = (9/8) \epsilon_0 \epsilon_r \mu_h (V^2/L^3)$, where ϵ_0 is the permittivity of free space, ϵ_r is the relative permittivity and assumed as approximately 3.0, μ_h is the hole mobility value, V is the effective voltage, L is the thickness of the active layer blend, and J is the current density. Atomic force microscopy (AFM) measurement of the active layer was carried out using DI Nanoscope Dimension 3100 atomic force microscope.

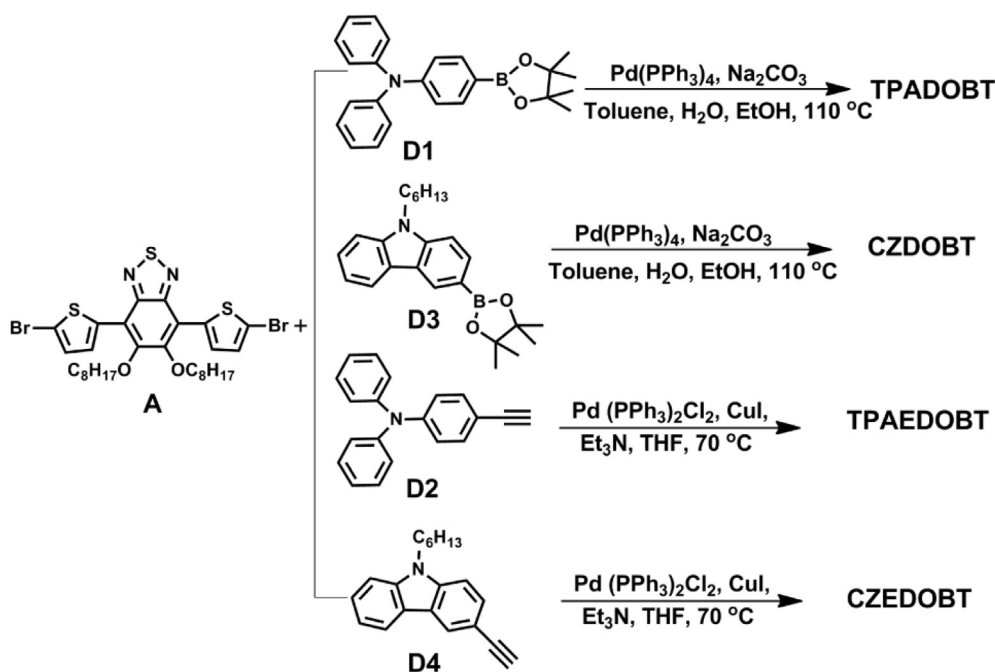
2.4. Synthesis and characterizations

The synthetic routes of the investigated compounds are shown in Scheme 2.

Compound A was prepared according to the procedure reported in the literature [9], and the synthetic details of compounds **D1**, **D2**,



Scheme 1. The molecular design strategy and chemical structures of **TPADOBT**, **CZDOBT**, **TPAEDOBT** and **CZE-DOBT**.



Scheme 2. Synthetic routes of TPADOBT, CZDOBT, TPAEOBT and CZEOBT.

D3 and **D4** are given in ESI [17]. The synthesis of **TPADOBT**, **CZDOBT**, **TPAEOBT** and **CZEOBT** are described in the following sections:

2.4.1. Synthesis of compound TPADOBT

A mixture of compound **D1** (184 mg, 0.5 mmol), compound **A** (178 mg, 0.25 mmol), Na_2CO_3 (848 mg, 8.0 mmol) and $\text{Pd}(\text{PPh}_3)_4$ (4 mg, 0.013 mmol) in a solution of toluene (8 mL), H_2O (4 mL) and EtOH (2 mL) was refluxed at 110 °C for 24 h. After being cooled to room temperature, the reaction solution was poured into 50 mL water, extracted with dichloromethane (DCM, 3 × 20 mL). The combined organic layer was dried over anhydrous sodium sulfate. The solvent was evaporated under reduced pressure and the residue was purified by column chromatography eluting with petroleum ether (PE): DCM (2:1, v/v) to give a purple solid (241 mg, yield: 92%), M.p.: 78–80 °C. ^1H NMR (400 MHz, CDCl_3 , ppm): δ 8.50 (d, $J = 1.2$ Hz, 2H), 7.58 (d, $J = 8.4$ Hz, 4H), 7.34 (d, $J = 1.6$ Hz, 2H), 7.28 (t, $J = 7.8$ Hz, 8H), 7.14 (d, $J = 7.6$ Hz, 8H), 7.09 (d, $J = 8.4$ Hz, 4H), 7.05 (t, $J = 7.2$ Hz, 4H), 4.16 (t, $J = 7.0$ Hz, 4H), 1.95–1.97 (m, 4H), 1.27–1.52 (m, 20H), 0.86 (t, $J = 6.8$ Hz, 6H). ^{13}C NMR (100 MHz, CDCl_3 , ppm): δ 151.61, 150.96, 147.49, 147.42, 145.50, 133.04, 131.92, 129.34, 128.50, 126.63, 124.62, 123.63, 123.18, 122.24, 117.43, 74.46, 31.85, 30.48, 29.60, 29.36, 26.14, 22.69, 14.12. HRMS (MALDI-TOF): 1042.4313, $[\text{M}^+]$ (calcd for $\text{C}_{66}\text{H}_{66}\text{N}_4\text{O}_2\text{S}_3$: 1042.4348).

2.4.2. Synthesis of compound CZDOBT

A mixture of compound **D3** (189 mg, 0.5 mmol), compound **A** (178 mg, 0.25 mmol), Na_2CO_3 (848 mg, 8.0 mmol) and $\text{Pd}(\text{PPh}_3)_4$ (4 mg, 0.013 mmol) in a solution of toluene (8 mL), 4 mL H_2O and 2 mL EtOH was refluxed at 110 °C for 24 h. After being cooled to room temperature, The reaction solution was poured into 50 mL water, extracted with DCM (3 × 20 mL) and the combined organic layer was dried over anhydrous sodium sulfate. The solvent was evaporated and the residue was purified by column chromatography on silica gel column eluting with PE: EA (2: 1, v/v) to give a red solid (211 mg, yield: 80%), M.p.: 86–89 °C. ^1H NMR (400 MHz, CDCl_3 , ppm): δ 8.45 (m, 4H), 8.17 (d, $J = 7.6$ Hz, 2H), 7.85 (s, 2H), 7.49 (t, $J = 7.6$ Hz, 4H), 7.43 (t, $J = 6.8$ Hz, 4H), 7.28 (s, 2H), 4.32 (s, 4H),

4.23 (t, $J = 7.0$ Hz, 4H), 1.90–2.03 (m, 8H), 1.27–1.58 (m, 32H), 0.86–0.90 (m, 12H). ^{13}C NMR (100 MHz, CDCl_3 , ppm): δ 151.65, 151.08, 140.98, 140.20, 131.98, 125.98, 125.67, 124.21, 123.40, 122.91, 121.99, 120.55, 119.09, 117.83, 117.49, 109.01, 108.92, 74.51, 43.27, 31.90, 31.60, 30.58, 29.69, 29.38, 29.01, 26.99, 26.19, 22.69, 22.56, 14.09, 14.01. HRMS (MALDI-TOF): 1054.5344, $[\text{M}^+]$ (calcd for $\text{C}_{66}\text{H}_{78}\text{N}_4\text{O}_2\text{S}_3$: 1054.5287).

2.4.3. Synthesis of compound TPAEOBT

A mixture of compound **A** (143 mg, 0.20 mmol), CuI (2 mg, 0.01 mmol), $\text{Pd}(\text{PPh}_3)_2\text{Cl}_2$ (4 mg, 0.005 mmol) and compound **D2** (135 mg, 0.5 mmol) in 20 mL THF and 15 mL Et_3N was refluxed at 70 °C for 12 h. The solvent was evaporated and the residue was purified by column chromatography on silica gel column eluting with PE: DCM (4: 1, v/v) to give a red solid (164 mg, yield: 75%), M.p.: 60–62 °C. ^1H NMR (400 MHz, CDCl_3 , ppm): δ 8.52 (d, $J = 4.0$ Hz, 2H), 7.39 (d, $J = 8.8$ Hz, 4H), 7.34 (d, $J = 4.0$ Hz, 2H), 7.29 (t, $J = 7.8$ Hz, 8H), 7.13 (d, $J = 7.6$ Hz, 8H), 7.08 (t, $J = 7.4$ Hz, 4H), 7.02 (d, $J = 8.8$ Hz, 4H), 4.14 (t, $J = 7.0$ Hz, 4H), 1.99–1.95 (m, 4H), 1.29–1.49 (m, 20H), 0.88 (t, $J = 6.6$ Hz, 6H). ^{13}C NMR (100 MHz, CDCl_3 , ppm): δ 151.93, 150.73, 148.11, 147.15, 135.28, 132.39, 131.36, 130.89, 129.43, 125.35, 125.09, 123.66, 122.16, 117.34, 115.74, 95.33, 82.42, 74.59, 31.83, 30.32, 29.50, 29.31, 25.97, 22.68, 14.11. HRMS (MALDI-TOF): 1090.4269 $[\text{M}^+]$ (calcd for $\text{C}_{70}\text{H}_{66}\text{N}_4\text{O}_2\text{S}_3$: 1090.4348).

2.4.4. Synthesis of compound CZEOBT

A mixture of compound **A** (143 mg, 0.20 mmol), CuI (2 mg, 0.01 mmol), $\text{Pd}(\text{PPh}_3)_2\text{Cl}_2$ (4 mg, 0.005 mmol), **D4** (137 mg, 0.5 mmol) in 20 mL THF and 15 mL Et_3N was refluxed at 70 °C for 24 h. The solvent was evaporated and the residue was purified by column chromatography on silica gel column eluting with PE: DCM (4: 1, v/v) to give a purple solid (132 mg, yield: 60%), M.p.: 75–80 °C. ^1H NMR (400 MHz, CDCl_3 , ppm): δ 8.56 (d, $J = 3.6$ Hz, 2H), 8.32 (s, 2H), 8.11 (d, $J = 7.6$ Hz, 2H), 7.65 (d, $J = 8.4$ Hz, 2H), 7.49 (t, $J = 7.6$ Hz, 2H), 7.37–7.42 (m, 6H), 7.27 (d, $J = 7.2$ Hz, 2H), 4.29 (t, $J = 7.2$ Hz, 4H), 4.19 (t, $J = 7.0$ Hz, 4H), 1.85–2.03 (m 8H), 1.26–1.55

(m, 32H), 0.85–0.89 (m, 12H). ^{13}C NMR (100 MHz, CDCl_3 , ppm): δ 151.93, 150.79, 140.85, 140.24, 135.07, 131.21, 130.91, 129.14, 126.16, 125.73, 123.95, 122.92, 122.49, 120.56, 119.41, 117.37, 112.96, 108.97, 108.80, 96.55, 81.37, 74.60, 43.26, 31.86, 31.56, 30.35, 29.54: 29.35, 28.95, 26.96, 26.00, 22.71, 22.55, 14.13, 14.00. HRMS (MALDI-TOF): 1102.5364 [M^+] (calcd for $\text{C}_{70}\text{H}_{78}\text{N}_4\text{O}_2\text{S}_3$: 1102.5287).

3. Results and discussion

3.1. Synthesis and thermal stability properties of materials

The synthetic routes of **TPADOBT**, **CZDOBT**, **TPAEDOBT** and **CZEDOBT** are outlined in Scheme 2. Starting from TPA and Cz, D1 and D3 were attained by Miyaura borylation reaction via bis(pinacolato)diborane with monobromo-substituted TPA and Cz, respectively, using potassium acetate as base and $\text{Pd}(\text{PPh}_3)_2\text{Cl}_2$ as catalyst in toluene. D2 and D4 were synthesized by Sonogashira cross-coupling reaction via ethynyltrimethylsilane with monoiodide-substituted TPA and Cz, respectively, in the presence of Et_3N , $\text{Pd}(\text{PPh}_3)_2\text{Cl}_2$ and CuI in THF, and more detailed synthetic procedure and characterization are described in Scheme S1 of ESI. The central DOBT-based acceptor unit of compound A was prepared according to previously reported procedure. Finally, **TPADOBT** and **CZDOBT** were synthesized by Pd-assisted Suzuki coupling reaction in high yields of 92% and 80%, respectively. **TPAEDOBT** and **CZEDOBT** were synthesized by Sonogashira coupling reaction in yields of 75% and 60%, respectively. Their chemical structures were determined with ^1H NMR, ^{13}C NMR and HRMS, which were consistent with their proposed structures. Four materials possess good solubility in common organic solvents, which meets the requirement for fabrication of solution-processed OPV devices. The thermal stability properties were studied by thermogravimetric analysis (TGA), as shown in Fig. S19 of ESI. The onset decomposition temperatures of **TPAEDOBT**, **CZEDOBT**, **TPADOBT** and **CZDOBT** with 5% weight-loss are 329 °C, 328 °C, 324 °C and 314 °C, respectively.

Accordingly, the exceptional thermal stability of these materials could provide a guarantee for their PV applications [18].

3.2. Optical properties

The solar absorption ability is preliminarily investigated with the UV–Vis absorption spectra of these compounds in chloroform solution and in thin film. As shown in Fig. 1, all compounds show two primary absorption bands at low and high energy region, covering 300–600 nm in solution and 300–700 nm in film respectively.

In solution, the quantitative UV–Vis absorption spectra of them were obtained in chloroform solution at a concentration of $1 \times 10^{-5} \text{ mol L}^{-1}$, as shown in Fig. 1(a). These compounds all present similar absorption spectra due to their similar D- π -A- π -D typed molecular backbone. The maxima absorption peaks ($\lambda_{\text{max}}^{\text{sol}}$) at low energy region of **TPAEDOBT**, **CZEDOBT**, **TPADOBT** and **CZDOBT** were observed at 511, 503, 522 and 520 nm, respectively, resulting from intermolecular charge transfer (ICT) transition between molecular terminal donor and central acceptor unit [19]. The pertinent molar extinction coefficient (ϵ) of them are listed in Table 1. As a consequence, the higher ϵ and stronger absorption were obtained for **TPAEDOBT** and **CZEDOBT** in comparison with another two single-bond compounds. The results indicate that the compounds with ethynyl-linker possess relatively stronger absorption capacity than single-bond compounds, probably contributing to the improvement of short-circuit current density (J_{SC}) [20]. By contrast, the absorption bands of these compounds in their thin film state are broadened and the absorption peaks ($\lambda_{\text{max}}^{\text{film}}$) are red-shifted by approximately 20 nm, suggesting the enhanced intermolecular interaction for solid-state packing [21]. The optical band gaps ($E_{\text{g}}^{\text{opt}}$) estimated from the absorption onsets of **TPAEDOBT**, **CZEDOBT**, **TPADOBT** and **CZDOBT** in film state are 2.04, 2.08, 2.00 and 2.05 eV respectively, which are in a desirable range for OPV applications [22].

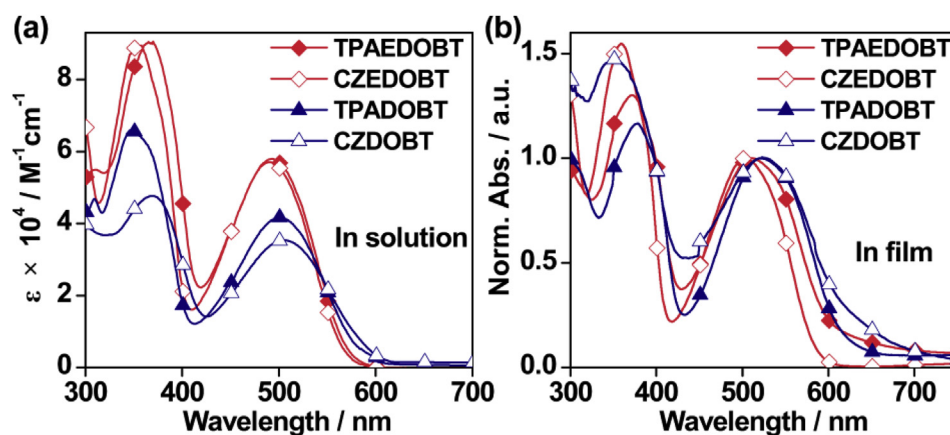


Fig. 1. (a) The quantitative UV–Vis absorption spectra of **TPADOBT**, **CZDOBT**, **TPAEDOBT** and **CZEDOBT** in chloroform solution at a concentration of $1 \times 10^{-5} \text{ mol L}^{-1}$; (b) UV–Vis absorption spectra of these compounds in thin films normalized in the region of long wavelength.

Table 1

The photophysical, electrochemical and theoretically calculated data of compounds **TPAEDOBT**, **CZEDOBT**, **TPADOBT** and **CZDOBT**.

	$\lambda_{\text{max}}^{\text{sol}}$ (nm)/ ϵ ($\text{M}^{-1} \text{ cm}^{-1}$)	$\lambda_{\text{max}}^{\text{film}}$ (nm)	$E_{\text{g}}^{\text{opt}}$ (eV)	K_{sv} (M^{-1})	HOMO ^{CV} (eV)	LUMO ^{CV} (eV)	E_{g}^{CV} (eV)	HOMO ^{DFT} (eV)	LUMO ^{DFT} (eV)	$E_{\text{g}}^{\text{DFT}}$ (eV)
TPAEDOBT	367/9.08, 495/5.81	511	2.04	3103	−5.29	−3.24	2.05	−4.66	−2.50	2.16
CZEDOBT	352/8.91, 493/5.67	503	2.08	3048	−5.31	−3.21	2.10	−4.67	−2.39	2.28
TPADOBT	372/6.55, 507/4.12	522	2.00	2984	−5.12	−3.15	1.97	−4.59	−2.35	2.24
CZDOBT	351/4.74, 499/3.52	520	2.05	2840	−5.14	−3.11	2.03	−4.63	−2.25	2.38

To evaluate the photoinduced charge separation process between donor and acceptor, the fluorescence quenching experiment was carried out with the synthesized donor materials and PC₆₁BM. As expected, the fluorescence quenching phenomenon of **TPAEDOB**, **CZEDOB**, **TPADOB** and **CZDOB** was clearly revealed. The fluorescence intensity of them gradually decreased with the increasing concentration of PC₆₁BM, as shown in Fig. 2, indicating an efficient charge separation process between the synthesized donors and acceptor PC₆₁BM. Moreover, the dependence of fluorescence intensity on the concentration of quencher PC₆₁BM is linear at low concentrations in conformity with the Stern-Volmer equation [23]: $F_0/F = 1 + K_{SV} [C]$, where F_0 and F represent the emission intensity in the absence and presence of PC₆₁BM, respectively, K_{SV} is the fluorescence quenching constant, and $[C]$ is the concentration of PC₆₁BM. According to Stern-Volmer equation, the fitting plots of these compounds are shown in inset of Fig. 2. Accordingly, the K_{SV} values of **TPAEDOB**, **CZEDOB**, **TPADOB** and **CZDOB** are 3103, 3048, 2984 and 2840 M⁻¹, respectively. All materials present high quenching constant, the efficient charge separation process is further approved. By contrast, the charge separation of **TPAEDOB** is more efficient relative to other three

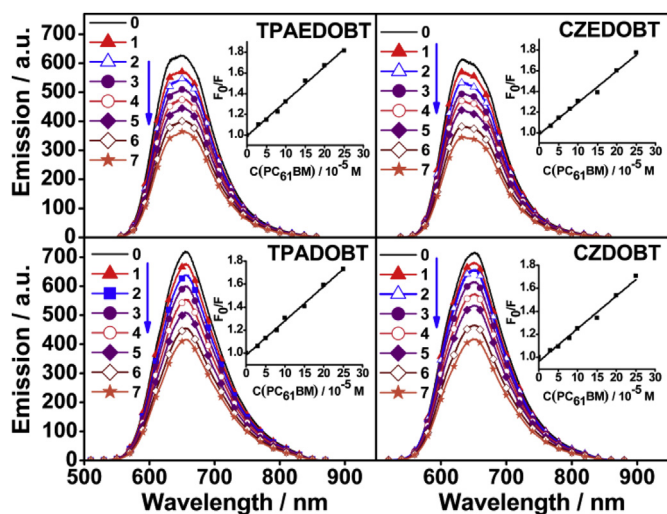


Fig. 2. Fluorescence emission spectra of donor materials **TPAEDOB**, **CZEDOB**, **TPADOB** and **CZDOB** in chloroform solution (1.0×10^{-5} M) with increasing concentration of acceptor PC₆₁BM ($\times 10^{-5}$ M): 0.0 (0), 3.0 (1), 5.0 (2), 8.0 (3), 10.0 (4), 15.0 (5), 20.0 (6), 25.0 (7); The insets are fitting plots for four compounds respectively by Stern-Volmer equation.

compounds due to its relatively higher K_{SV} value, probably contributing to its enhanced PV performance.

3.3. Electrochemical characteristics

Cyclic voltammetry (CV) experiment was performed to investigate the electrochemical property and energy levels of these compounds (measurement details are recorded in experimental section). The cyclic voltammogram of them in 0.1 M Bu₄NBF₄/CH₂Cl₂ solution are shown in Fig. 3, and the corresponding electrochemical data are summarized in Table 1. The onset oxidation potential (E_{ox}) at 0.37 and 0.39 V is obtained in the anode potential region for single-bond compounds **TPADOB** and **CZDOB**, corresponding to the oxidation of TPA and Cz unit, respectively. By contrast, the triple-bond compounds **TPAEDOB** and **CZEDOB** exhibit the greatly increased E_{ox} at 0.54 and 0.56 V, respectively, attributing to the electron-withdrawing character of ethynyl-linker [24]. In addition, a slightly increased E_{ox} is observed for compounds **CZDOB** and **CZEDOB** with weakened electron-donating unit (Cz) relative to **TPADOB** and **TPAEDOB**. On the other hand, the onset reduction potentials (E_{red}) at -1.60 and -1.64 V is observed in the cathodic potential region for **TPADOB** and **CZDOB** respectively, corresponding to the reduction of DOBT. In contrast to two single-bond compounds, **TPAEDOB** and **CZEDOB** exhibit the greatly increased E_{red} at -1.51 and -1.54 V respectively, also attributing to the electron-withdrawing character of ethynyl-linker. In contrast to the reduction behaviour of **TPADOB** and **TPAEDOB**, a slightly increased E_{red} is observed for compounds **CZDOB** and **CZEDOB** owing to the weakened electron-donating unit (Cz). As a result, the increasing of oxidation and reduction potential values of **TPAEDOB** and **CZEDOB** relative to **TPADOB** and **CZDOB** can be rationally attributed to the molecular design with ethynyl-linker. The electrochemical band gaps (E_g^{CV}) and the corresponding energy levels (HOMO^{CV} and LUMO^{CV}) could be achieved from E_{ox} and E_{red} (calculation details are described in experimental section). Consequently, the HOMO^{CV} levels for **TPAEDOB**, **CZEDOB**, **TPADOB** and **CZDOB** are -5.29 , -5.31 , -5.12 and -5.14 eV, and their LUMO^{CV} levels are -3.24 , -3.21 , -3.15 and -3.11 eV, respectively. These data indicate that ethynyl-linker is very effective in lowering both the HOMO and LUMO levels of the materials without significantly costing their narrow band gaps [25]. The electrochemical energy-level diagram of these compounds together with PC₆₁BM was schematically shown in Fig. S20 of ESI. The results clearly demonstrate that all these compounds in principle can behave as donor materials with PC₆₁BM as acceptor in solution-processed OPV cells [26]. By contrast, **TPAEDOB** and **CZEDOB** possess

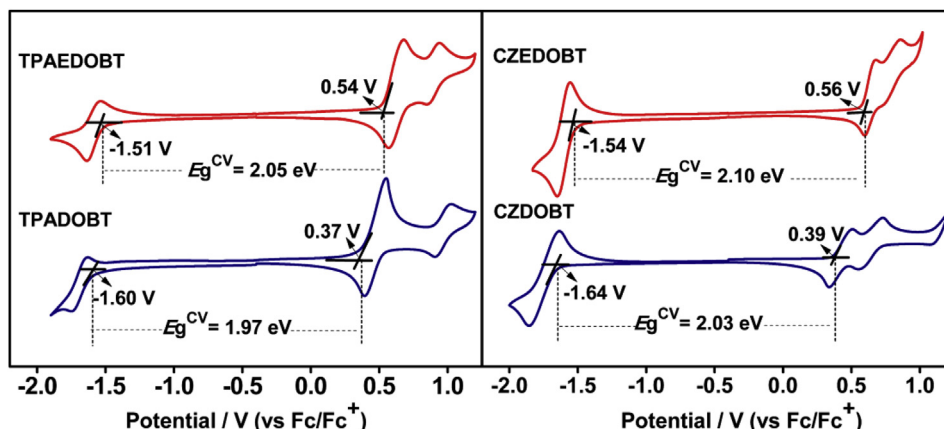


Fig. 3. Cyclic voltammogram of **TPAEDOB**, **CZEDOB**, **TPADOB** and **CZDOB** in 0.1 M Bu₄NBF₄/CH₂Cl₂ solution under nitrogen atmosphere with a scan rate of 100 mV s⁻¹.

obviously lower HOMO^{CV} levels, which could probably ensure the high V_{OC} . Among them, **CZEDOBT** exhibits a lowest HOMO^{CV} level in contrast to the other three compounds, which should be attributed to the synergistic effect of ethynyl-linker and relatively weakened electron-donating ability of Cz units. Herein, remarkably improvement of V_{OC} values in **CZEDOBT** based device will be expected. Moreover, their E_g^{CV} are estimated to be about 2.05, 2.10, 1.97 and 2.03 eV, respectively, which are in good agreement with their optical band gaps.

3.4. Theoretical calculations

In order to further demonstrate the strategy of molecular design, the density functional theory (DFT) and the time-dependent density functional theory (TD-DFT) calculations were performed on these compounds to analyze their molecular orbital depictions, energy levels, electronic transitions and optical absorption profiles using Gaussian 09 software at the Becke's three-parameter gradient-corrected functional (B3LYP) with a polarized 6-31G(d) basis [27]. A summary of the computational analysis for **TPAEDOBT**, **CZEDOBT**, **TPADOBT** and **CZDOBT** using DFT/TD-DFT methods is illustrated in Fig. 4, and the calculated data of energy levels (HOMO^{DFT} and LUMO^{DFT}) and band gaps (E_g^{DFT}) are also summarized in Table 1. Fig. 4(a), clearly presents the schematic diagram of the calculated energy levels, frontier molecular orbital and electronic-density distributions of these molecules. The electronic densities of HOMO are similarly distributed the entire molecular backbone without a significant biased distribution, whereas those of LUMO are predominantly located on the central DOBT, revealing an apparent ICT process between molecular terminal donor and central acceptor unit [28]. Moreover, the electronic densities of HOMO-1 are located on their terminal electron-donating groups with a greater proportion. This feature reveals that the terminal donor unit could

probably play an important role in stabilizing of separated hole from excitons and thus improve the hole transporting capacity [29]. The calculated HOMO^{DFT} for **TPAEDOBT**, **CZEDOBT**, **TPADOBT** and **CZDOBT** are -4.66 , -4.67 , -4.59 and -4.63 eV, and the corresponding LUMO^{DFT} are -2.50 , -2.39 , -2.35 and -2.25 eV, respectively. Thus the HOMO^{DFT} values for **TPAEDOBT** and **CZEDOBT** decreased 0.07 and 0.04 eV, while the LUMO^{DFT} values also reduced 0.15 and 0.14 eV in contrast to that of **TPADOBT** and **CZDOBT**. These results imply that HOMO and LUMO energy levels can be reduced simultaneously without sacrificing the E_g via incorporating ethynyl-linker on molecular backbone, which could potentially contribute to the V_{OC} and J_{SC} [30]. Despite the discrepancies exist between computational analysis and experimental results, theoretical calculations for a series of closely related materials have proven to be crucial to understanding the strategy of molecular design [31].

The calculated optical absorption profiles and electronic transitions of **TPAEDOBT**, **CZEDOBT**, **TPADOBT** and **CZDOBT** are shown in Fig. 4(b), and the calculated data of electronic transitions using TD-DFT method are summarized in Table S1 of ESI. The predicted absorption spectra of these compounds show two primary bands at short and long wavelength, which are consistent with their UV–Vis absorption spectra. The long wavelength absorption band correlates with the electron transition between the HOMO and LUMO, while the short one is primarily a result of HOMO to LUMO+1 transition. Despite with some margin of error in TD-DFT predicted profiles, the trend could be reliably computed for these closely related compounds [32]. These results could preliminarily guide the strategy of molecular design.

3.5. Hole mobility

Hole-mobility (μ_h) is often considered as one of the most important physical parameters for donor material design. The μ_h of

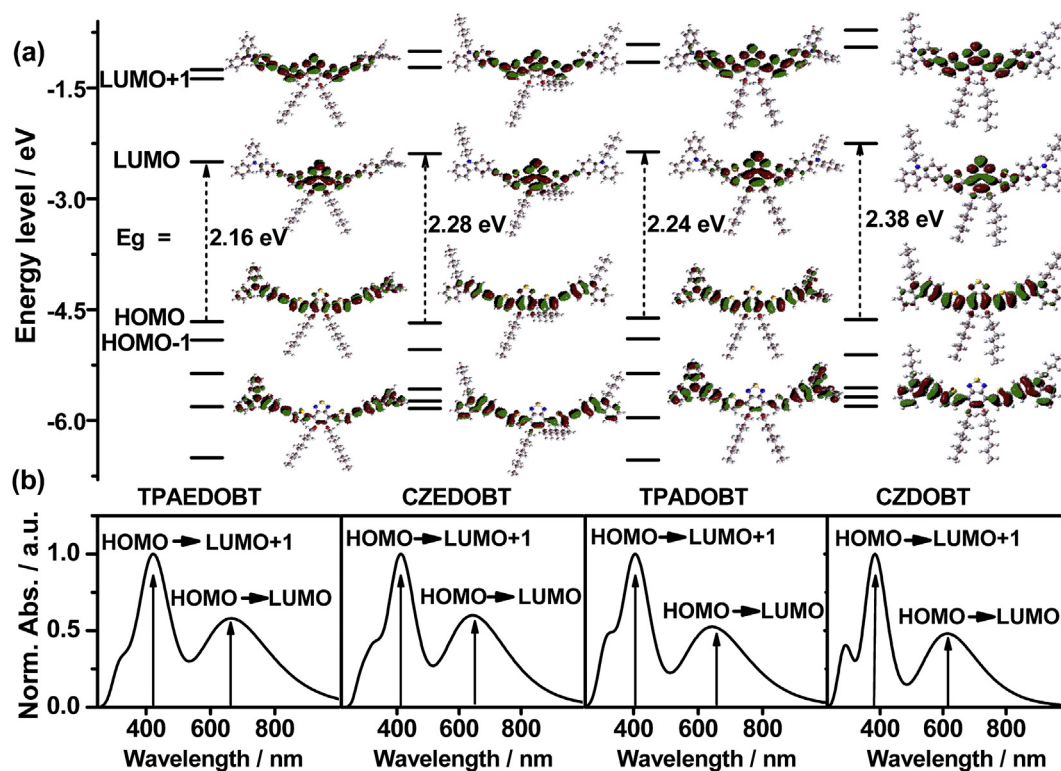


Fig. 4. Summary of the computational analysis for **TPAEDOBT**, **CZEDOBT**, **TPADOBT** and **CZDOBT** using DFT/TD-DFT methods. (a) calculated energy levels, molecular orbital depictions and electronic-density distributions; (b) predicted optical absorption profiles and calculated electronic transitions.

each material was achieved in the dark with a structure of ITO/PEDOT:PSS/SMs-donor:PC₆₁BM/Au, as shown in Fig. 5. As you can see, the *J*-*V* curves of hole-only devices were recorded in Fig. 5(a) and the μ_h values can be determined in a double logarithmic scale by fitting the *J*-*V* curves to a SCLC model using the Mott-Gurney law (the method is described in experimental section). Accordingly, the fitting plots of the data points in ohmic regime and in SCLC regime are depicted in Fig. 5(b), and the μ_h values can be obtained in the SCLC region with a slope of 2 [33]. As listed in Table 2, the derived μ_h values of TPAEDOBT, CZEDOBT, TPADOBT and CZDOBT are 1.32×10^{-3} , 6.00×10^{-4} , 3.60×10^{-4} and 5.65×10^{-5} cm² V⁻¹ s⁻¹, respectively.

As literature reported, the hole-transporting capacity of PV-donor materials might be closely related to their unique chemical structure and the intermolecular interaction of solid film [34]. As expected, the μ_h values of TPAEDOBT and CZEDOBT are much greater than those of TPADOBT and CZDOBT, indicating that the triple-bond compounds possess much favoured molecular structure and enhanced intermolecular interaction induced by improved coplanarity and rigidity with ethynyl-linker. By contrast, TPAEDOBT-based device possesses the optimal hole transporting capacity in accordance with its greatest μ_h value among them. Supplementary evidence could be provided by its relatively higher degree of crystallinity from X-ray diffraction analysis (XRD patterns are shown in Fig. S21 of ESI). The results would probably provide some valuable hints on their PV performance, especially the *J*_{SC} and PCEs.

3.6. Photovoltaic properties

To fully evaluate the PV property of new materials and reveal the relations between the property and molecular structure, a series of BHJ devices with a typical architecture of ITO/PEDOT:PSS/SMs-donor:PC₆₁BM/Au were fabricated in chloroform solution. We first performed the optimization of the devices based on SMs-donor:PC₆₁BM blends with varied D/A weight ratios (1:1, 1:2 and 1:3). Accordingly, the data of PV performance are summarized in Table S2 of the ESI documents. Remarkably, the device with the D/A weight ratio of 1:2 showed the best PV performance for each material. The related current density voltage (*J*-*V*) characteristics of the PV devices with the D/A weight ratio of 1:2 are sketched in Fig. 6, and the pertinent device parameters are listed in Table 2. As a result, the *J*_{SC} of TPAEDOBT, CZEDOBT, TPADOBT and CZDOBT are 8.35, 6.68, 5.93 and 5.66 mA cm⁻², respectively. By contrast, the

Table 2

The hole mobility data and PV parameters of the devices based on TPAEDOBT, CZEDOBT, TPADOBT and CZDOBT.

	μ_h (cm ² V ⁻¹ s ⁻¹)	<i>V</i> _{OC} (V)	<i>J</i> _{SC} (mA cm ⁻²)	FF	PCE (%)
TPAEDOBT	1.32×10^{-3}	1.01	8.35	0.38	3.21
CZEDOBT	6.00×10^{-4}	1.06	6.68	0.30	2.10
TPADOBT	3.60×10^{-4}	0.92	5.93	0.34	1.85
CZDOBT	5.65×10^{-5}	0.95	5.66	0.34	1.82

relatively higher *J*_{SC} values of triple-bond compounds could be rationally attributed to their relatively higher molar extinction coefficients and more efficient carrier transporting capacity. This result is consistent with their UV–Vis absorption and their hole mobility. Meanwhile, the relatively higher *J*_{SC} values of TPA-based compounds relative to Cz-based compounds can be also assigned to the relatively narrower *E*_g, higher ϵ and μ_h values. In contrast to 0.92 V of TPADOBT and 0.95 V of CZDOBT, the increased *V*_{OC} values of 1.01 and 1.06 V are achieved for the devices based on TPAEDOBT and CZEDOBT, respectively. The higher *V*_{OC} values result from their relatively higher electrochemical *E*_{ox} and deeper-lying HOMO levels induced by rational molecular design.

It is worth mentioning that an impressive *V*_{OC} of 1.06 V has been observed for CZEDOBT-based device most likely due to synergistic effect of ethynyl-bridge with the electron-withdrawing character and Cz units with the relatively weakened electron-donating ability. Moreover, the PCEs of 1.85% and 1.82% were obtained for single-bond compounds TPADOBT and CZDOBT. While the devices based on triple-bond compounds TPAEDOBT and CZEDOBT exhibited a superior PCE of 3.21% and 2.10% respectively. Remarkably among them, the best PV performance was obtained for TPAEDOBT-based device, most likely arising from its triple-bond effect and its remarkably high hole transporting capacity, since a consistent trend was observed for their PCEs and μ_h values. Bearing in mind that the morphology of the active layer also has important effect on the performance of device. AFM measurement was carried out to investigate the morphology properties and the interesting results were revealed. TPAEDOBT exhibited relatively higher *J*_{SC}, FF and PCE values, which were consistent with its better bicontinuous interpenetrating networks as shown in AFM image. On the contrary, CZDOBT with the worse morphology exhibited relatively lower PCE value (ESI, Fig. S22).

In order to further verify PV performance, the IPCE spectra of related devices based on TPAEDOBT, CZEDOBT, TPADOBT and CZDOBT were tested as well. As shown in Fig. 6(b), all spectra

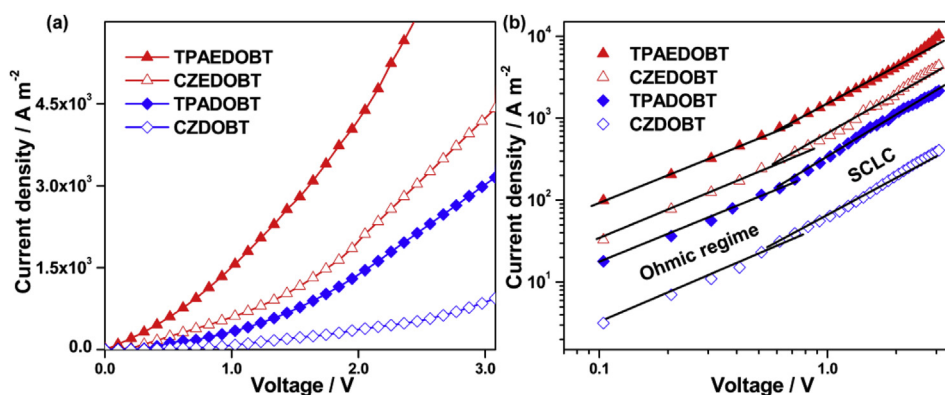


Fig. 5. Hole mobility of the compounds TPAEDOBT, CZEDOBT, TPADOBT and CZDOBT. (a) *J*-*V* curves of the hole-only devices tested in the dark with an architecture of ITO/PEDOT:PSS/SMs-donor:PC₆₁BM (1:2, w:w)/Au; (b) *J*-*V* curves of the devices in a double logarithmic scale, and the solid lines are fitting plots of the data points in ohmic regime and in SCLC regime.

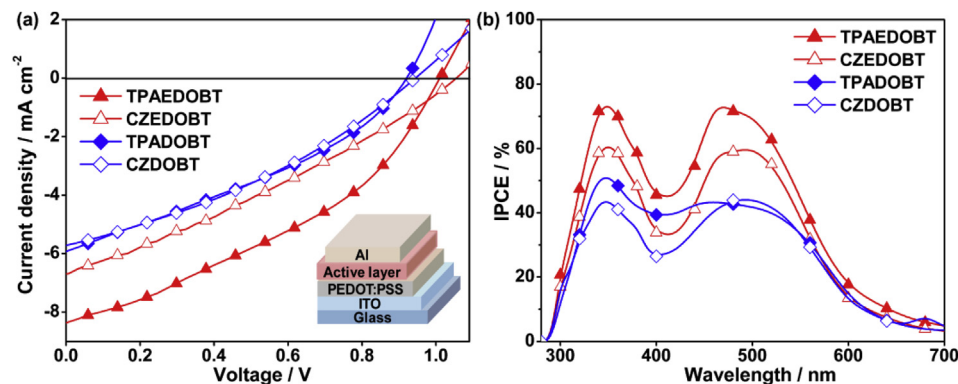


Fig. 6. PV properties of the investigated compounds **TPAEDOBt**, **CZEDOBt**, **TPADOBt** and **CZDOBt**. (a) *J*-*V* characteristics of the PV devices with a structure of ITO/PEDOT: PSS/SMS-donor:PC₆₁BM (1: 2, w: w)/Al under an illumination of AM 1.5G (100 mW cm⁻²). Inset: schematic structure of PV device; (b) The IPCE spectra of the devices.

exhibit a first peak around 350 nm followed by a second broad band with maximum value at around 490 nm, which are in agreement with their absorption profiles. A first maximum of ca. 72%, 60%, 50% and 43% in the region of 300–400 nm and a second maximum of ca. 72%, 59%, 42% and 44% in the region of 400–700 nm were obtained for **TPAEDOBt**, **CZEDOBt**, **TPADOBt** and **CZDOBt**, respectively. As a result, the IPCE values show consistent trend with their *J*_{SC} values. Among them, the higher IPCE values were obtained for devices based on **TPAEDOBt** and **CZEDOBt** compared to those of two reference compounds. In particular, it is worth pointing out that **TPAEDOBt** based device showed a highest IPCE value, which is responsible for its best *J*_{SC} and PCE in comparison. All integrated *J*_{SC} values from the IPCE spectra show within 5% mismatch compared with the *J*_{SC} from the *J*-*V* curves. Further experimental work on device optimization are underway in our team.

4. Conclusions

In conclusion, a series of novel D- π -A- π -D typed DOBT-based dyes named **TPAEDOBt**, **CZEDOBt**, **TPADOBt** and **CZDOBt** have been designed and synthesized successfully for solution-processable BHJ-OSCs. Their PV properties were finely tuned via the molecular design with ethynyl-linker and terminal electron-donating units. By contrast, the relatively high PCE of 3.21% has been achieved for **TPAEDOBt**-based device due to its triple-bond effect and high hole-mobility capacity. Most importantly, a remarkably increased *V*_{oc} of 1.06 V has been obtained for **CZEDOBt**-based device due to the synergistic effect of ethynyl-linker with electron-withdrawing character and Cz units with the relatively weakened electron-donating ability, which is among the earliest report for DOBT-Cz based SMs with high *V*_{oc} so far. The results provide the valuable hints for rational design of novel SMS-donor materials.

Acknowledgements

This work was supported by funds from the NSFC (No. 21102013, 21471024, 21101020, 21071025), the SRF for ROCS-SEM (201001438, 201001439), the RFD (20090041120017) and the Fundamental Funds for the Central Universities (No. DUT16ZD205, DUT11LK20, DUT15LK20 and DUT15ZD118).

Appendix A. Supplementary data

Supplementary data related to this article can be found at <http://dx.doi.org/10.1016/j.dyepig.2017.01.044>.

References

- (a) Mishra A, Bauerle P. Small molecule organic semiconductors on the move: promises for future solar energy technology. *Angew Chem Int Ed* 2012;51(9): 2020–67.
(b) Walker B, Kim C, Nguyen T-Q. Small molecule solution-processed bulk heterojunction solar cells. *Chem Mater* 2011;23(3):470–82.
- (a) Chen J-D, Cui C, Li Y-Q, Zhou L, Ou Q-D, Li C, et al. Single-junction polymer solar cells exceeding 10% power conversion efficiency. *Adv Mater* 2015;27(6): 1035–41.
(b) He Z, Xiao B, Liu F, Wu H, Yang Y, Xiao S, et al. Single-junction polymer solar cells with high efficiency and photovoltage. *Nat Photon* 2015;9:174–9.
(c) Liu Y, Zhao J, Li Z, Mu C, Ma W, Hu H, et al. Aggregation and morphology control enables multiple cases of high-efficiency polymer solar cells. *Nat Commun* 2014;5:5293–301.
(d) Yu W, Huang L, Yang D, Fu P, Zhou L, Zhang J, et al. Efficiency exceeding 10% for inverted polymer solar cells with a ZnO/ionic liquid combined cathode interfacial layer. *J Mater Chem A* 2015;3:10660–5.
- (a) Chen Y, Wan X, Long G. High performance photovoltaic applications using solution-processed small molecules. *Acc Chem Res* 2013;46(11):2645–55.
(b) Wu R, Yin L, Li Y. II-Linkage effect of push-pull-structure organic small molecules for photovoltaic application. *Sci China Mater* 2016;59(5):371–88.
- (a) Liu Y, Chen C-C, Hong Z, Gao J, Yang YM, Zhou H, et al. Solution-processed small-molecule solar cells: breaking the 10% power conversion efficiency. *Sci Rep* 2013;3:3356–64.
(b) Kan B, Zhang Q, Li M, Wan X, Ni W, Long G, et al. Solution-processed organic solar cells based on dialkylthiol-substituted benzodithiophene unit with efficiency near 10%. *J Am Chem Soc* 2014;136(44):15529–32.
(c) Cui C, Guo X, Min J, Guo B, Cheng X, Zhang M, et al. High-performance organic solar cells based on a small molecule with alkylthio-thienyl-conjugated side chains without extra treatments. *Adv Mater* 2015;27(45): 7469–75.
- Kan B, Li M, Zhang Q, Liu F, Wan X, Wang Y, et al. A series of simple oligomer-like small molecules based on oligothiophenes for solution-processed solar cells with high efficiency. *J Am Chem Soc* 2015;137(11):3886–93.
- Liu X, Chen H, Tann S. Overview of high-efficiency organic photovoltaic materials and devices. *Renew Sustain Energy Rev* 2015;52:1527–38.
- (a) Yang M, Pan C, Chen X, Liu B, Zou Y, Zhong H. A solution-processable D-A-D small molecule based on isoindigo for organic solar cells. *J Mater Sci* 2012;48(3):1014–20.
(b) Dutta P, Park H, Lee W-H, Kang I-N, Lee S-H. A crystalline D- π -A organic small molecule with naphtho[1,2-b:5,6-b']dithiophene-core for solution processed organic solar cells. *Org Electron* 2012;13(12):3183–94.
(c) Shang H, Fan H, Shi Q, Li S, Li Y, Zhan X. Solution processable D-A-D molecules based on triphenylamine for efficient organic solar cells. *Sol Energy Mater Sol Cells* 2010;94(3):457–64.
(d) Pan J-Y, Zuo L-J, Hu X-L, Fu W-F, Chen M-R, Fu L, et al. Star-shaped D-A small molecules based on diketopyrrolopyrrole and triphenylamine for efficient solution-processed organic solar cells. *ACS Appl Mater Interfaces* 2013;5(3):972–80.
- Zhou J, Wan X, Liu Y, Zuo Y, Li Z, He G, et al. Small molecules based on benzo [1,2-b:4,5-b']dithiophene unit for high-performance solution-processed organic solar cells. *J Am Chem Soc* 2012;134(39):16345–51.
- Zeng S, Yin L, Ji C, Jiang X, Li K, Li Y, et al. D- π -A- π -D type benzothiadiazole-triphenylamine based small molecules containing cyano on the π -bridge for solution-processed organic solar cells with high open-circuit voltage. *Chem Commun* 2012;48(86):10627–9.
- Wang L, Yin L, Ji C, Li Y. Tuning the photovoltaic performance of BT-TPA chromophore based solution-processed solar cells through molecular design incorporating of bithiophene unit and fluorine-substitution. *Dye Pigm* 2015;118:37–44.

- [11] (a) Liu Q, Zhan H, Ho C-L, Dai F-R, Fu Y, Xie Z, et al. Oligothiophene-bridged bis(arylene ethynylene) small molecules for solution-processible organic solar cells with high open-circuit voltage. *Chem Asian J* 2013;8:1892–900.
(b) Mun J-W, Cho I, Lee D, Yoon WS, Kwon OK, Lee C, et al. Acetylene-bridged D-A-D type small molecule comprising pyrene and diketopyrrolopyrrole for high efficiency organic solar cells. *Org Electron* 2013;14(9):2341–7.
(c) Vybornyi O, Jiang Y, Baert F, Demeter D, Roncali J, Blanchard P, et al. Solution-processable thienoisindigo-based molecular donors for organic solar cells with high open-circuit voltage. *Dye Pigment* 2015;115:17–22.
- [12] Zhang C-H, Wang L-P, Tan W-Y, Wu S-P, Liu X-P, Yu P-P, et al. Effective modulation of aryl acetylenic molecular system based on dithienyldiketopyrrolopyrrole for organic solar cells. *J Mater Chem C* 2016;4:3757–64.
- [13] Wang L, Yin L, Ji C, Zhang Y, Gao H, Li Y. High open-circuit voltage of the solution-processed organic solar cells based on benzothiadiazole-triphenylamine small molecules incorporating π -linkage. *Org Electron* 2014;15(6):1138–48.
- [14] (a) Zhou P, Dang D, Xiao M, Wang Q, Zhong J, Tan H, et al. Improved photovoltaic performance of star-shaped molecules with a triphenylamine core by tuning the substituted position of the carbazolyl unit at the terminal. *J Mater Chem A* 2015;3:10883–9.
(b) Casey A, Ashraf RS, Fei Z, Heeney M. Thioalkyl-substituted benzothiadiazole acceptors: copolymerization with carbazole affords polymers with large Stokes shifts and high solar cell voltages. *Macromolecules* 2014;47(7):2279–88.
(c) Dutta P, Kim J, Eom SH, Lee W-H, Kang IN, Lee S-H. An easily accessible donor- π -acceptor-conjugated small molecule from a 4,8-dialkoxybenzo[1,2-b:4,5-b']dithiophene unit for efficient solution-processed organic solar cells. *ACS Appl Mater Interfaces* 2012;4(12):6669–75.
- [15] Du C, Li C, Li W, Chen X, Bo Z, Veit C, et al. 9-Alkylidene-9H-fluorene-containing polymer for high-efficiency polymer solar cells. *Macromolecules* 2011;44(19):7617–24.
- [16] Paek S, Cho N, Song K, Jun M-J, Lee JK, Ko J. Efficient organic semiconductors containing fluorine-substituted benzothiadiazole for solution-processed small molecule organic solar cells. *J Phys Chem C* 2012;116(44):23205–13.
- [17] (a) Paramasivam M, Gupta A, Raynor AM, Bhosale SV, Bhanuprakash K, Rao VJ. Small band gap D- π -A- π -D benzothiadiazole derivatives with low-lying HOMO levels as potential donors for applications in organic photovoltaics: a combined experimental and theoretical investigation. *RSC Adv* 2014;4:35318–31.
(b) Castro E, Cabrera-Espinoza A, Deemer E, Echegoyen L. Low-energy-gap organic based acceptor-donor-acceptor π -conjugated small molecules for bulk-heterojunction organic solar cells. *Eur J Org Chem* 2015;2015(21):4629–34.
(c) Ji C, Yin L, Wang L, Jia T, Meng S, Sun Y, et al. Linkage effects of linear D- π -A- π -D diketopyrrolopyrrole-triphenylamine based solution-processable organic small molecule photovoltaic materials. *J Mater Chem C* 2014;2(20):4019–26.
- [18] Kim J-H, Kim HU, Kang I-N, Lee SK, Moon S-J, Shin WS, et al. Incorporation of pyrene units to improve hole mobility in conjugated polymers for organic solar cells. *Macromolecules* 2012;45(21):8628–38.
- [19] Jadhav T, Misra R, Biswas S, Sharma GD. Bulk heterojunction organic solar cells based on carbazole-BODIPY conjugate small molecules as donors with high open circuit voltage. *Phys Chem Chem Phys* 2015;17:26580–8.
- [20] Shen S, Jiang P, He C, Zhang J, Shen P, Zhang Y, et al. Solution-processable organic molecule photovoltaic materials with bithienyl-benzodithiophene central unit and indenedione end groups. *Chem Mater* 2013;25(11):2274–81.
- [21] Mazzio KA, Yuan M, Okamoto K, Luscombe CK. Oligoselenophene derivatives functionalized with a diketopyrrolopyrrole core for molecular bulk heterojunction solar cells. *ACS Appl Mater Interfaces* 2011;3(2):271–8.
- [22] He G, Wan X, Li Z, Zhang Q, Long G, Liu Y, et al. Impact of fluorinated end groups on the properties of acceptor-donor-acceptor type oligothiophenes for solution-processed photovoltaic cells. *J Mater Chem C* 2014;2(7):1337–45.
- [23] (a) Wang J, Wang D, Moses D, Heeger AJ. Dynamic quenching of 5-(2'-ethylhexyloxy)-p-phenylene vinylene (MEH-PPV) by charge transfer to a C60 derivative in solution. *J Appl Polym Sci* 2001;82:2553–7.
(b) Zhao T, Liu Z, Song Y, Xu W, Zhang D, Zhu D. Novel diethynylcarbazole macrocycles: synthesis and optoelectronic properties. *J Org Chem* 2006;71:7422–32.
(c) Wang J, Wang D, Miller EK, Moses D, Bazan GC, Heeger AJ. Photoluminescence of water-soluble conjugated polymers: origin of enhanced quenching by charge transfer. *Macromolecules* 2000;33:5153–8.
- [24] (a) Wu X-F, Fu W-F, Xu Z, Shi M, Liu F, Chen H-Z, et al. Spiro linkage as an alternative strategy for promising nonfullerene acceptors in organic solar cells. *Adv Funct Mater* 2015;25(37):5954–66.
(b) Gao H, Li Y, Wang L, Ji C, Wang Y, Tian W, et al. High performance asymmetrical push-pull small molecules end-capped with cyanophenyl for solution-processed solar cells. *Chem Commun* 2014;50:10251–4.
- [25] (a) Boudreault P-LT, Hennek JW, Loser S, Ortiz RP, Eckstein BJ, Facchetti A, et al. New semiconductors based on 2,2'-ethyne-1,2-diyldis[3-(alk-1-yn-1-yl)thiophene] for organic opto-electronics. *Chem Mater* 2012;24(15):2929–42.
(b) Du C, Li W, Li C, Bo Z. Ethynylene-containing donor-acceptor alternating conjugated polymers: synthesis and photovoltaic properties. *J Polym Sci Part A Polym Chem* 2013;51(2):383–93.
- [26] Zhang L, Zeng S, Yin L, Ji C, Li K, Li Y, et al. The synthesis and photovoltaic properties of A-D-A-type small molecules containing diketopyrrolopyrrole terminal units. *New J Chem* 2013;37(3):632–9.
- [27] Chen R, Wang Y, Chen T, Li H, Zheng C, Yuan K, et al. Heteroatom-bridged benzothiazolyls for organic solar cells: a theoretical study. *J Phys Chem B* 2015;119(2):583–91.
- [28] Wang X, Sun Y, Chen S, Guo X, Zhang M, Li X, et al. Effects of π -conjugated bridges on photovoltaic properties of donor- π -acceptor conjugated copolymers. *Macromolecules* 2012;45(3):1208–16.
- [29] Gautam P, Misra R, Koukaras EN, Sharma A, Sharma GD. Donor-acceptor-acceptor-donor small molecules for solution processed bulk heterojunction solar cells. *Org Electron* 2015;27:72–83.
- [30] Stuart AC, Tumbleston JR, Zhou H, Li W, Liu S, Ade H, et al. Fluorine substituents reduce charge recombination and drive structure and morphology development in polymer solar cells. *J Am Chem Soc* 2013;135(5):1806–15.
- [31] Liu Q, Liu Y, Wang Y, Ai L, Ouyang X, Han L, et al. Anthradithiophene-benzothiadiazole-based small molecule donors for organic solar cells. *New J Chem* 2013;37(11):3627–33.
- [32] Wang D, Zhang X, Ding W, Zhao X, Geng Z. Density functional theory design and characterization of D-A-A type electron donors with narrow band gap for small-molecule organic solar cells. *Comput Theor Chem* 2014;1029:68–78.
- [33] (a) Liang Y, Feng D, Wu Y, Tsai S-T, Li G, Ray C, et al. Highly efficient solar cell polymers developed via fine-tuning of structural and electronic properties. *J Am Chem Soc* 2009;131:7792–9.
(b) Mihailitchi VD, Xie HX, de Boer B, Koster LJA, Blom PWM. Charge transport and photocurrent generation in poly(3-hexylthiophene): methanofullerene bulk-heterojunction solar cells. *Adv Funct Mater* 2006;16(5):699–770.
- [34] (a) Wang E, Ma Z, Zhang Z, Vandewal K, Henriksson P, Inganäs O, et al. An easily accessible isoindigo-based polymer for high-performance polymer solar cells. *J Am Chem Soc* 2011;133(36):14244–7.
(b) Liu B, Chen X, Zou Y, Xiao L, Xu X, He Y, et al. Benzo[1,2-b:4,5-b']difuran-Based Donor-Acceptor copolymers for polymer solar cells. *Macromolecules* 2012;45:6898–905.